UNITED NATIONS UNIVERSITY
UNU-GTP
Geothermal Training Programme

Orkustofnun, Grensasvegur 9,
IS-108 Reykjavik, Iceland

Reports 2018
Number 20

# WELL DESIGN FOR THE ASAL GEOTHERMAL FIELD: A CASE STUDY FOR WELL GLC-2

**Mouhoumed Mahamoud Ahmed**
Djibouti Development Office of Geothermal Energy (ODDEG)
PK20, Zone Industriel, Raod National N° 1
Djibouti
REPUBLIC OF DJIBOUTI
*moud826@gmail.com*

## ABSTRACT

The purpose of this report is to prepare a well design for a future well, namely GLC-2 located in the Asal geothermal Field, Djibouti. Existing well lithology data was referred to in order to prepare the well design. The wells Asal 1, Asal 3 and Asal 6 are among the producing wells in the Asal geothermal field and they have a close lithological relationship. The wells Asal 3 and Asal 6 produce highly saline (about 120 g/l) reservoir fluid. Consequently, the BPD curve for 12 wt% NaCl salt water was used and it influences also the effective containment pressure. The curve was then used for the determination of minimum casing setting depths. The planned depth of the well is 2000 m and the resulting minimum depth of the production casing is set at 1100 m with an 8-1/2" production section down to 2000 m, and the anchor and the surface casings have minimum setting depths of 670 m and 400 m, respectively. Casing stresses during the drilling operation and production phase were evaluated according to the method indicated in the African Union Code of Practice for Geothermal Drilling. The sizes of the casings are 20", 13 3/8" and 9 5/8", and based on the calculations the weight was selected as 94 lb/ft, 68 lbf, 43.5 lb/ft, respectively. The selected casings are of material grade K-55, which is a grade recommended for geothermal wells. The density of the water and cement is 0.988 kg/l and 1.617 kg/l respectively. The maximum pressure (effective containment pressure) in the well is 14 bars. To ensure the casing design of the well, the data was used to assess the axial, radial and hoop stresses generated by the temperature, to the applied pressure or static pressure. The casings were selected based on design factors that were higher than the minimum design factors indicated in the African Code of Practice for Geothermal Drilling.

## 1. INTRODUCTION

Geothermal well design is one of the most important activities before the drilling phase of geothermal wells. Proper well design aims at ensuring the successful extraction of the hot geothermal fluid from the reservoir. The goal of the well design is to successfully extract maximum power (steam) to the surface without causing damage to the interior equipment (casing, joints and liner,) and surface equipment (wellhead, flange, expansion spool, etc.) as well as avoiding hazard to personnel. To avoid damage to equipment and ensure protection of personnel during drilling operations and production of the well, rules and regulations related to drilling such as the African Union Code of Practice for Geothermal Drilling (African Union, 2016) should be followed.

Previous pre-feasibility and feasibility studies of geothermal exploration in the Asal rift area showed positive results for geothermal exploitation. There are seven wells drilled in the Asal geothermal field. The first two wells Asal 1 and Asal 2 were drilled in 1975 (BRGM, 1975). Four additional wells Asal 3, Asal 4, Asal 5 and Asal 6 were later drilled in same area in 1989 (Aquater, 1989). Three of the wells; Asal 1, Asal 3 and Asal 6 proved productive. However, the wells produced highly saline fluids due to reservoir contamination with saline water from Lake Asal (Jalludin, 2013).

As an example, the production rate of Asal 3 has been estimated at 200 t/h at 20 bar and the fluid at reservoir conditions has a temperature of 261°C and salinity of about 120 g/l (Aquater, 1989). The objective of the current study is to (i) prepare the design of a well that is planned close to Asal wells 3 and 6, (ii) develop a well drilling programme and wellhead.

## 2. THE ASAL GEOTHERMAL FIELD

### 2.1 Geography

The Asal area is located in the middle of the Republic of Djibouti (Figure 1). The Asal geothermal field is in the Asal Rift area on the isthmus between Lake Asal and Ghoubet al Kharab Gulf (Figure 1). The Asal rift is located 120 km north of Djibouti city which is 155 m below sea level (Árnason, 2008).

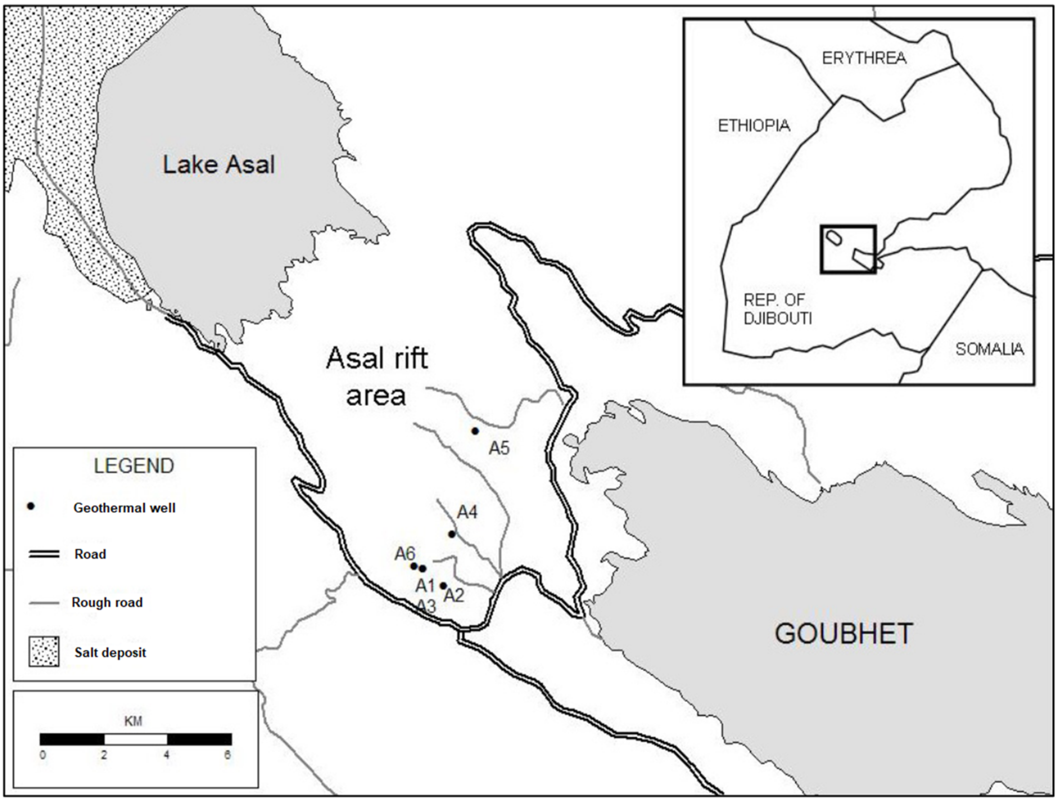


FIGURE 1: Location of the Asal region and geothermal boreholes in the Asal Rift area (Elmi, 2005)

The region is an arid desert, with an average rainfall of 79 mm per year. Hydrogeological studies of the region show a general groundwater flow toward Lake Asal, which is the lowest point of the area, and is occupied by a salt lake saturated in sodium chloride and calcium sulphates (Elmi, 2005).

**2.2 Geology**

Before detailing the geology of the Asal rift, the general geology of the Republic of Djibouti is discussed.

The Republic of Djibouti is located in East Africa, where three major extensional structures, the Red sea, the East African Rift and the Gulf of Aden, join to form the Afar depression (Figure 2). This depression is bounded by large escarpments to the west and to the south and by the Danakil Alps to the northeast. Almost all of the Republic of Djibouti is covered by volcanic rocks and thermal manifestation are widespread (Bosch et al., 1974). The most active structure in the Afar depression is the Asal Rift, which is the westward extension of the Gulf of Aden-Gulf of Tadjoura Ridge.

The Asal Rift geology is characterized by flat lying lava flows, generally erupted through a series of vents on an open fissure. The most recent volcanic eruption took place at Ardoukoba, southeast of Lake Asal in 1978. This volcanic eruption lasted only a week. The rift is about 9-10 km wide and is bounded to the southwest and northeast by impressive normal faults (Árnason et al., 2008). Additionally, the region has a few hot springs located along the edge faults of the collapse. Due to this geological situation, the geothermal gradient is particularly high in the Asal rift zone and explains why this area was chosen for the implementation of geothermal energy projects. Very recent volcanic rocks dominate the Asal rift zone. They are listed in order from the surface as (Demange and Puvilland, 1993):

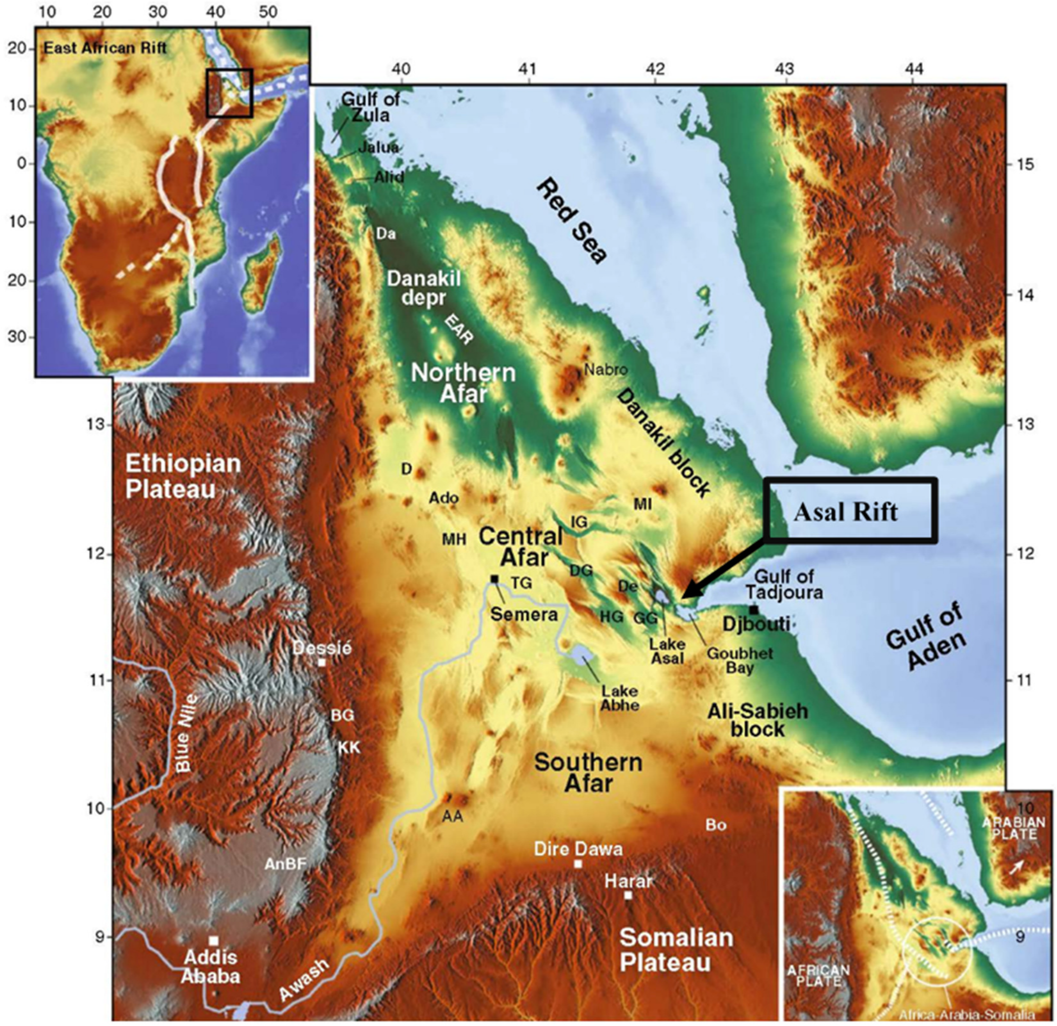


FIGURE 2: Regional setting of the Asal Rift (Geologica, 2016).

- Recent basalt flows (Asal series);
- Hyaloclastites (Asal series);
- Basalt (Gulf series);
- Rhyolites (age of the order of 1 MA); and
- Dalha basalt series (age of 4 to 7 MA).

## 2.3 Well information

During geothermal exploration, seven wells have been drilled to date: Asal 1 and Asal 2 were drilled by BRGM in 1975 and Asal 3, Asal 4, Asal 5 and Asal 6 were drilled by Interdril, Ltd. and supervised by Aquater during 1987 and 1988 (for location see Figure 3). The last well drilled was GLC-1 in 2016. Further details on depth, recorded temperature, mass flow and salinity of the wells are shown in Table 1. The seventh well is GLC-1, which was drilled to a depth of 600 m, and had a temperature of 138°C.

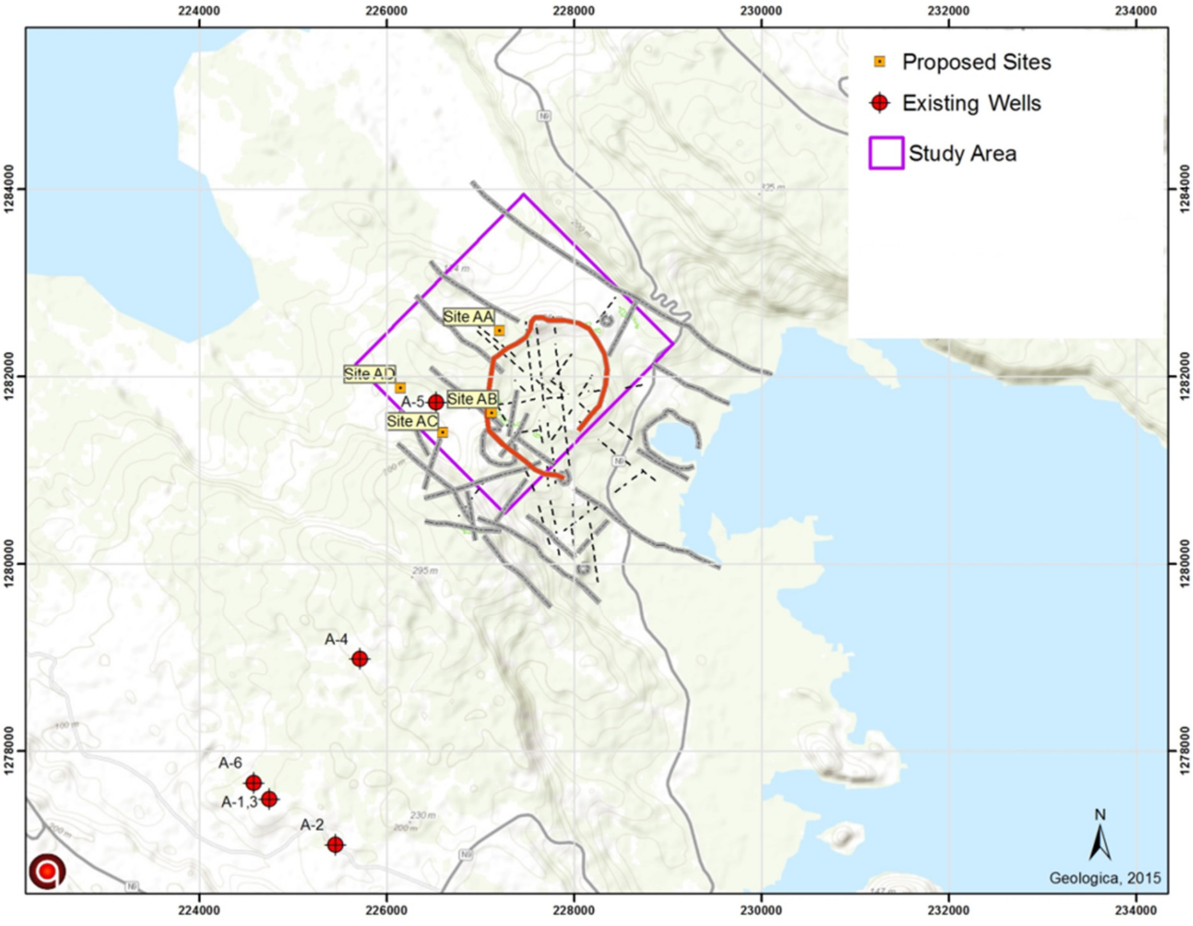


FIGURE 3: Topographical map showing the study area (Geologica, 2016)

TABLE 1: Characteristics of old Asal wells drilled in the 1970s and 1980s (Ali, 2015)

| Name | Drilling | | Final depth (m) | Bottom temperature (°C) | Mass flow (t/h) | Salinity (g/l) |
|---|---|---|---|---|---|---|
| | Start | End | | | | |
| Asal 1 | 08.03.1975 | 12.06.1975 | 1146 | 260 | 135 | 120 |
| Asal 2 | 01.07.1975 | 10.09.1975 | 1554 | 233 (926 m) | - | - |
| Asal 3 | 11.06.1987 | 11.09.1987 | 1316 | 264 | 350 | 130 |
| Asal 4 | 15.09.1987 | 21.12.1987 | 2013 | 359 | - | 180 |
| Asal 5 | 07.01.1988 | 07.03.1988 | 2105 | 359 | - | - |
| Asal 6 | 08.04.1988 | 10.07.1988 | 1761 | 265 | 150 | 130 |

Exploration drilling has not been completed in the Asal area. In the beginning of August 2018, drilling contractor Iceland Drilling (IDC) started drilling at a site near the Asal 5 well and ICD plans to drill three exploration wells in the same Asal zone with well depths of 2000 m to 2800 m.

The drilling sites for the new wells were decided based on a pre-feasibility study done by ÍSOR – Iceland GeoSurvey (Reykjavik Energy Invest, 2008). Figure 3 shows a topographical map of the study area, previously drilled wells, faults/fractures, the Fiale caldera, surface geothermal manifestations, and previously proposed drilling sites. Djibouti N9 road is displayed in grey.

## 2.4 Well production

Three of the drilled wells Asal 1, Asal 3 and Asal 6 proved productive. The Asal 2, Asal 4 and Asal 5 wells have poor permeability despite having a temperatures range of 253-359°C. In the 1000-1300 m range, the three producing wells crossed the basaltic series of Dalha, which holds a high-temperature liquid-dominated geothermal system with a temperature of 260°C, and produces a geothermal brine with a salinity of 116 g/l in the reservoir.

Production test data from the three producing wells, Asal 1, Asal 3 and Asal 6 demonstrated the existence of a geothermal reservoir with a good permeability thickness, kh = 6-16 Dm, as well as the existence of significant sulphite and silica incrustation phenomena (Virkir-Orkint, 1990).

The Asal Rift is characterized by a diverging plate boundary that has accumulated a substantial volume of basaltic magma. Microseismicity is persistent while large earthquakes are few. A correlation of stratigraphic units between the different Asal wells is presented below in the form of a synthetic scheme (Figure 4). The correlation between the different lithological units of the wells begins at the surface down to a depth of 1500 m. The distribution of volcanic formations on the different boreholes are:

The three producing wells have a coherence of different lithological units compared to the other Asal

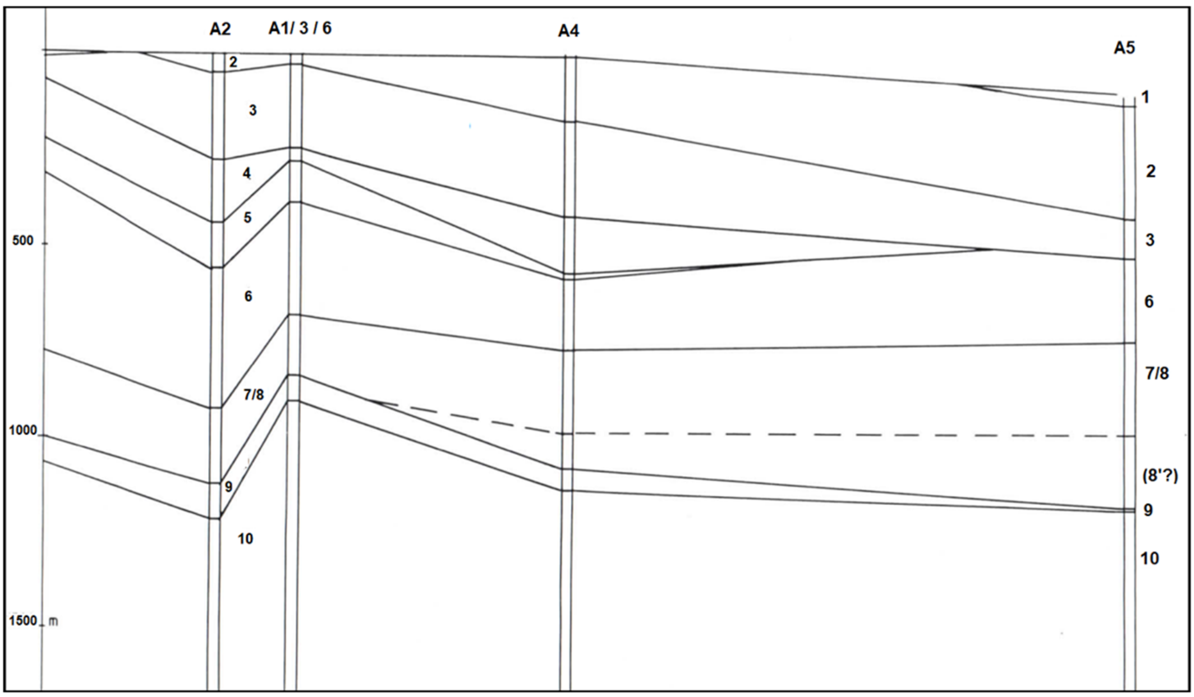


FIGURE 4: Correlation of stratigraphy between different wells (Demange and Puvilland, 1993); 1: Asal axial zone, 2: Central Asal, 3: Extreme margins of Asal, 4: Initial series of Asal Tdajoura, 5: Pleistocene sediments, 6: Eger Aleyta acid series (s-I), 7: Stratoid series, 8: Pliocene sediments, 9: Dalha series, 10: Acid series of Mabla

wells since they are close to each other.

The lithology of the Asal 3 well (Figure 5) is taken as a reference in the casing part programme as well as its dynamic pressure (Figure 6) and the dynamic temperature (Figure 7). At a depth of 1200 m, the pressure and temperature of the wellhead are 90 bar and 265°C, respectively.

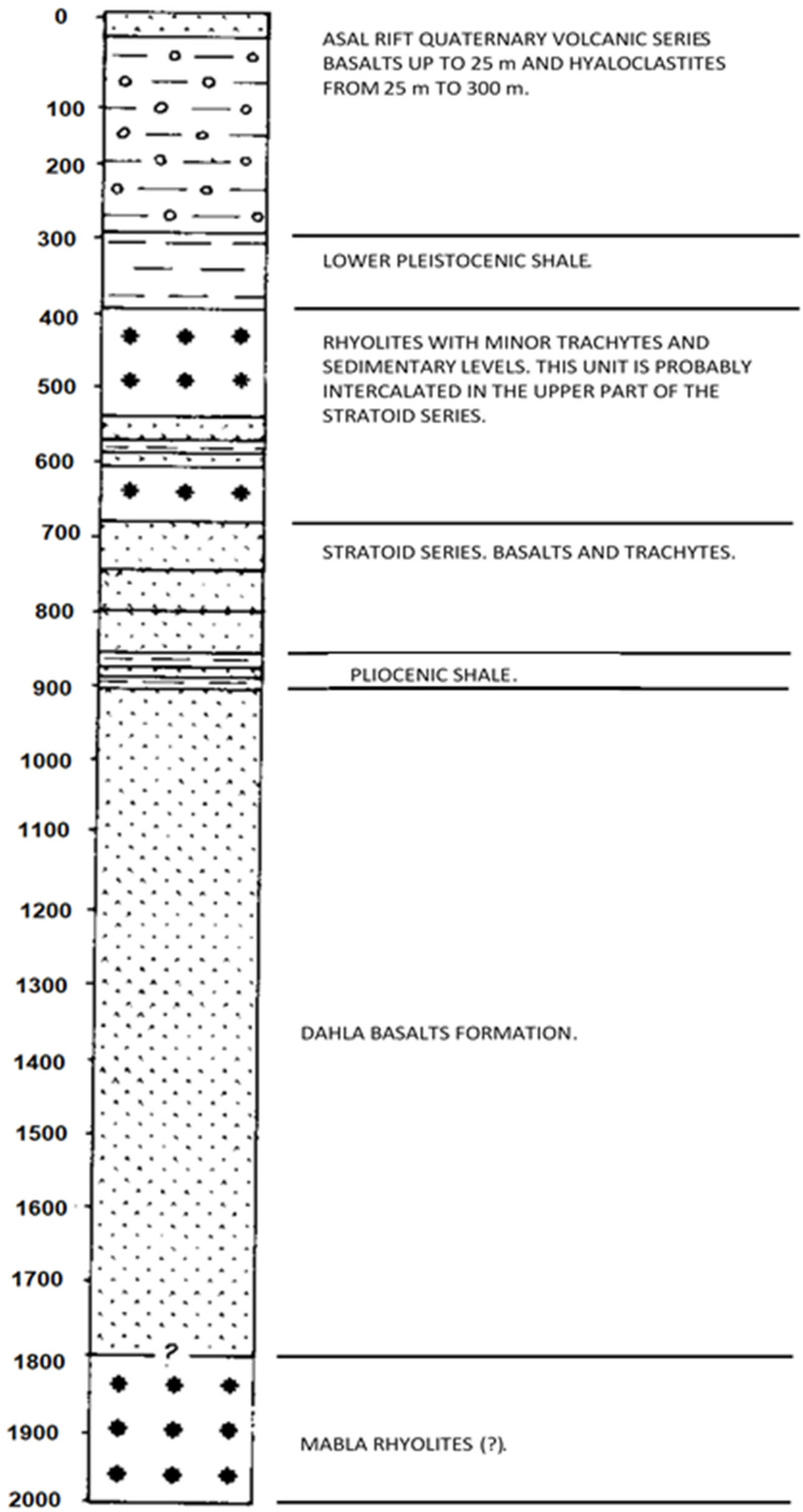


FIGURE 5: Stratigraphic column of well Asal 3

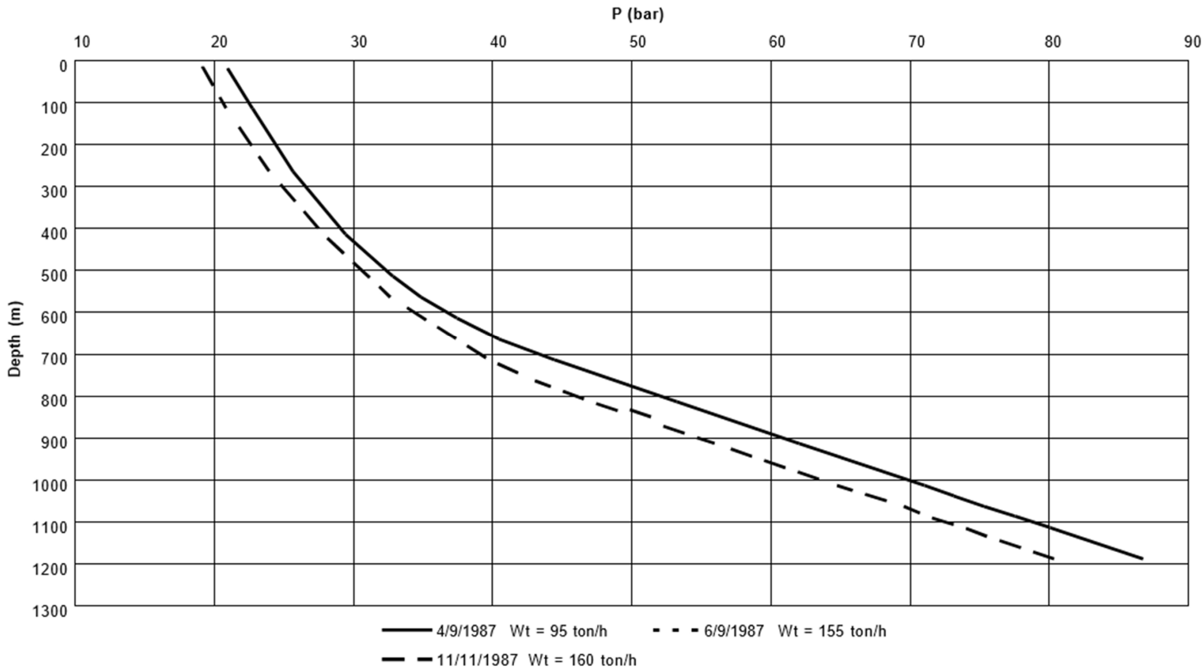


FIGURE 6: Pressure profiles during discharge testing of well Asal 3 (Elmi, 2005)

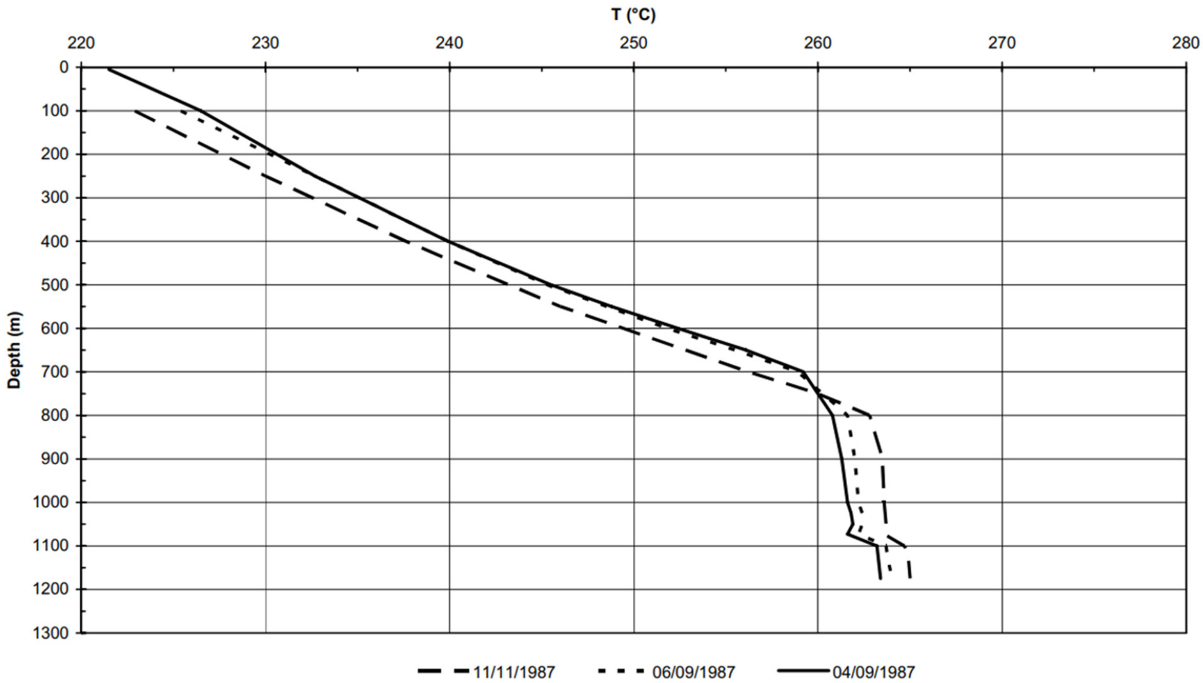


FIGURE 7: Temperature profiles during discharge testing well Asal 3 (Elmi, 2005)

## 3. CASING DESIGN

In this section a casing programmeme for a future well in the Asal geothermal field is proposed. As mentioned before, the future well is planned approximately between the wells Asal 3 and Asal 6. For determining the minimum casing shoe depths, the lithology of the Asal 3 well is used as a reference. This should be revised when location of the well has been selected. For each casing string, various load cases are considered consisting of casing stress conditions of tri-axial, axial and hoop components.

In order to complete the design of a future well and avoid the risks associated with drilling deep geothermal wells guidelines of the African Union Code of Practice for Geothermal Drilling (African Union, 2016) were applied.

### 3.1 Minimum casing setting depth

The selection of casing string and setting depth is based on the formation pore pressure and fracture gradient of the well. In this case the well Asal 3 is used as a reference. The minimum casing setting depth design is evaluated between the effective containment pressure (fracture gradient of the well Asal 3) and boiling-point-for-depth (BPD) pressure assuming 120 g/l saline fluid (formation pore pressure).

For the casing setting depth determination, the effective containment pressure and the BPD curve for 12wt% NaCl is described in Figure 8. The maximum wellhead pressure is estimated as 140 bar assuming a static column of steam from the bottom of the well (Figure 9).

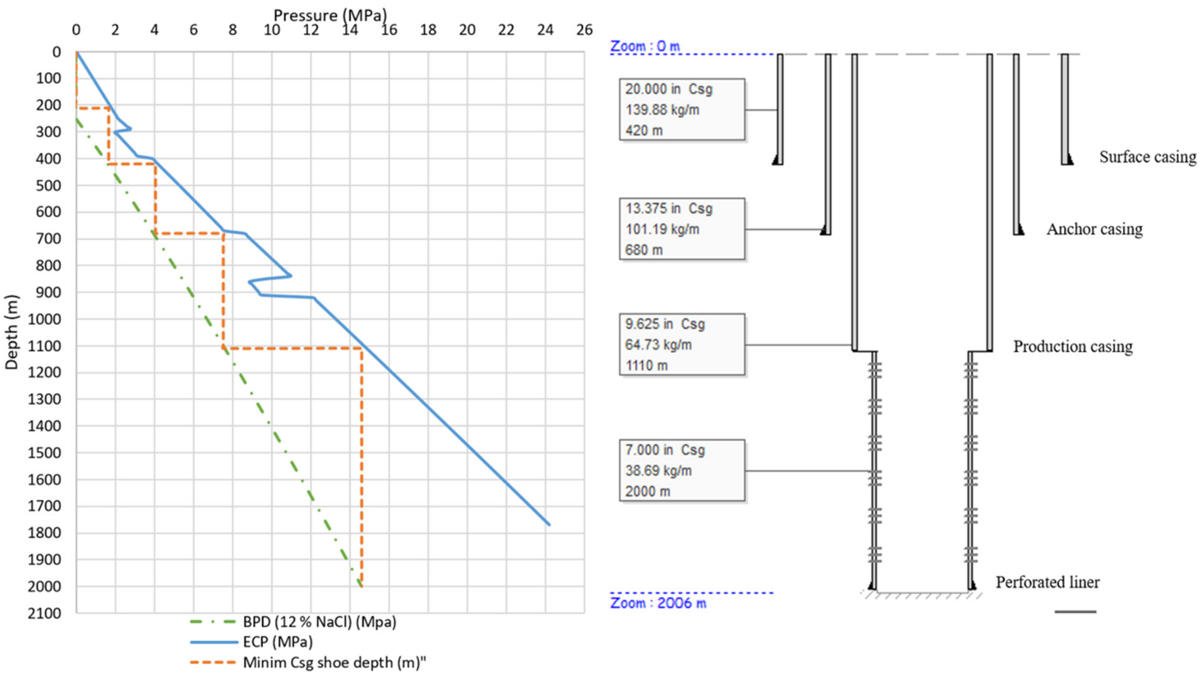


FIGURE 8: Minimum setting depths according to method described in African Union (2016) and the resulting casing programme with casing depths of 420, 680 and 1110 m

An estimation of formation fracture pressure is found using the Eaton formula (Equations 1 and 2):

$$P_{frac} = P_f + \frac{v}{1-v}(S_V - P_f) \tag{1}$$

$$S_V = \rho_r g h \tag{2}$$

where $P_{frac}$ = Fracture pressure of a formation [MPa];
$P_f$ = Pore pressure [MPa];
$v$ = Poisson's ratio;
$S_V$ = Overburden pressure [MPa];
$\rho_r$ = Density of rock [kg/ m$^3$];
$g$ = Acceleration due to gravity (9.81 [m/ s$^2$]); and
$h$ = Depth of rock [m].

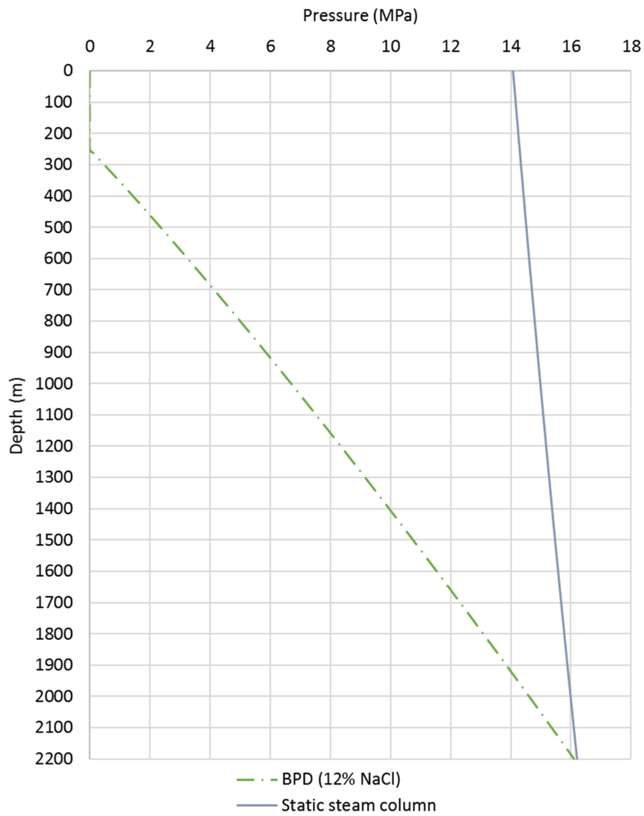


FIGURE 9: The maximum wellhead pressure of 144 bar (14 MPa) assuming saturated steam coming from 2000 m depth; the maximum wellhead temperature is assumed to be 336°C, the saturation temperature at 144 bar

## 3.2 Casing stress

### 3.2.1 Triaxial stress

In this section, the triaxial stress is assessed. The triaxial stress is the combined effects of all the principal stresses in a general stress state; axial stress, hoop stress and radial stress, shown in Figure 10. Triaxial stress (equivalent stress) is not a true stress; it is a theoretical value that allows a generalized three-dimensional (3D) stress state to be compared with a uniaxial failure criterion (the yield strength).

The triaxial safety factor is the ratio of the material´s yield strength to the triaxial stress. The yielding criterion is stated as:

$$\sigma_{VME} = \frac{1}{\sqrt{2}} \sqrt{(\sigma_a - \sigma_h)^2 + (\sigma_h - \sigma_r)^2 + (\sigma_r - \sigma_a)^2} \geq Yp \tag{3}$$

where $\sigma_{VME}$ = Differential pressure on casing during cementing [MPa];
$\sigma_a$ = Axial stress [psi];
$\sigma_h$ = Hoop or tangential stress [psi]; and
$\sigma_r$ = Radial stress [psi].

For triaxial design the design factor is:

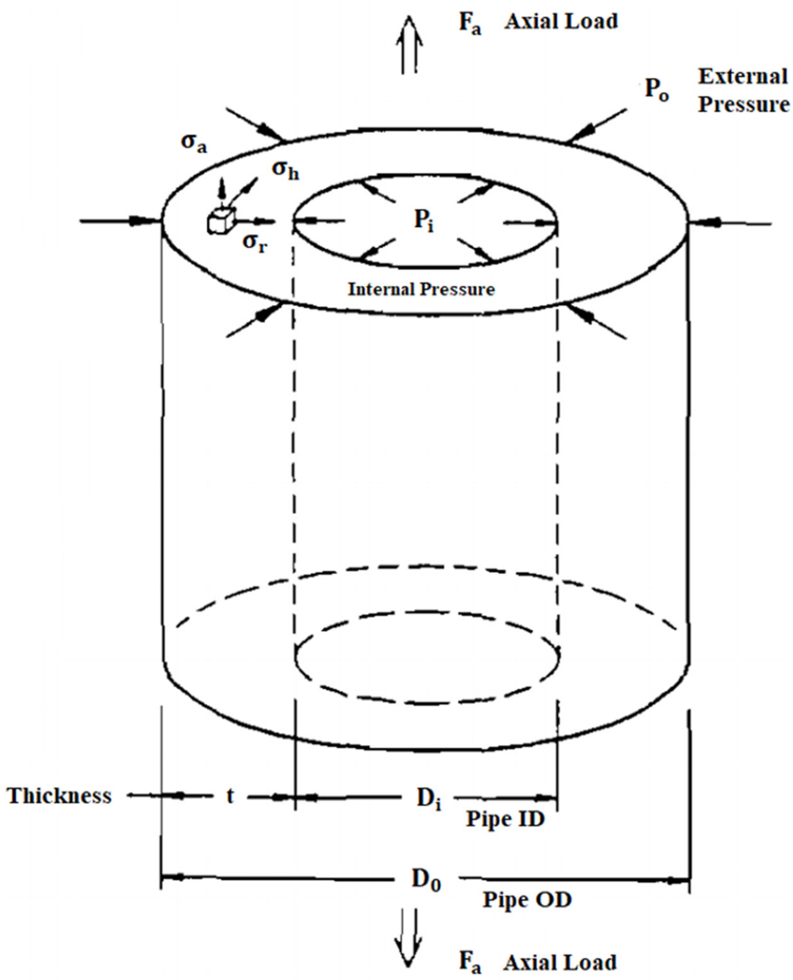


FIGURE 10: The casing stress (Maurer Engineering, Inc., 1993); $D_0$ = Pipe outer diameter [in]; $D_i$ = Pipe inner diameter [in]; $\sigma_a$ = Yield stress axial [psi]; $\sigma_h$ = Yield stress hoop [psi]; $\sigma_r$ = Yield stress radial [psi]; $P_i$ = Internal pressure [psi]; $P_o$ = External pressure [psi]; and $F_a$ = Axial load [lb]

$$\frac{\sigma_y}{\sigma_t} \geq 1.25 \tag{4}$$

where $\sigma_y$ = Minimum material yield stress [psi]; and
$\sigma_t$ = Maximum total equivalent triaxial stress [psi].

Alternatively, the triaxial stress is calculated, calculating each individual stress using the methods in the African Union Code of Practice for Geothermal Drilling (African Union, 2016).

### 3.2.2 Axial stress

The axial loads can be tensile or compressive. In the case of a geothermal well casing, the axial load was caused by the casing weight, temperature and well pressure. These parameters may be present before and after cementing the casing. As the first step, the tensile force during running and cementing the casing is evaluated using Equation 5. The axial load applied before cementing is evaluated by:

$$F_{hookhand} = F_{csg\ air\ wt} + F_{csg\ contents} - F_{displaced\ fluids} \tag{5}$$

where $F_{csg\ air\ wt}$ = Air weight of casing [kN];

$F_{csg\ contents}$ = Weight of internal contents of casing [kN]; and
$F_{displaced\ fluids}$ = Weight of fluids displaced by casing [kN].

The design factor is:

$$\frac{\sigma_{tm}}{F_{tm}} \geq 1.8 \tag{6}$$

where $\sigma_{tm}$ = Minimum tensile strength [psi]; and
$F_{tm}$ = Minimum axial load [kN].

The axial loading imposed after cementing shall be checked for applicability and magnitude near both the top and the shoe of the casing string.

Among the axial forces after cementing there is the fluid lifting force on anchor casing. The lifting force is met at the top with a force of opposite direction, which is generally dependent on the wellhead weight as in order for the wellhead to remain in place, a tension must be provided that anchors it. The tension, $P_w$ [MPa] occurring at the top of any string that anchors a wellhead against the lifting force applied by the fluid in the well is:

$$F_w = \frac{\pi}{4} \times P_w \times d^2 \times 10^{-3} - F_m \tag{7}$$

where $P_w$ = Maximum wellhead pressure [MPa];
$d$ = Casing inside diameter [mm]; and
$F_m$ = Net downward force applied by the wellhead due to its own mass and pipework reaction [kN].

The maximal pressure and the saturation temperature, which are 14.4 bar and 336°C, respectively (Figure 8) are used for determining the flange and valve conforming to ANSI and to API. The result is ANSI 1500.

After the calculation of the lifting force, it must be checked that the tensile strength of the anchor casing (13 3/8") can withstand the lifting force. The design factor is:

$$\frac{\sigma_{tm}}{F_{tm}} \geq 1.8$$

where $\sigma_{tm}$ = Minimum tensile strength;
$F_{tm}$ = Maximum axial load.

There is another axial force after cementing that can be applied to the anchor casing by the thermal expansion of another casing string where the production casing is poorly cemented inside the anchor casing and its tip reaches the casing head flange. Therefore, an increase or decrease in the temperature will result in additional compressive or tensile stress. Decrease in the surrounding temperature causes a change in the axial tension according to:

$$F_C = E.a\,(T_1 - T_2)A_p \times 10^{-3} \tag{8}$$

$$F_r = F_p - F_C \tag{9}$$

where $F_C$ = Change in axial force within casing body due to heating [kN];
$E$ = Modulus of elasticity [MPa];
$a$ = Coefficient of thermal expansion [°C];
$T_1$ = Neutral temperature (temperature of casing at time of cement set [°C] ;
$T_2$ = Maximum expected temperature [°C];

$A_p$ = Cross-sectional area of casing wall (mm$^2$), allowing for any slotting;
$F_r$ = Resultant axial force within casing body, combining the force at cement set and subsequent thermal forces [kN];
$F_p$ = Axial force within casing body at cement set [kN].

The design factor is:

$$\frac{\sigma_{t\ acs}}{\sigma_{c\ rcs}} \geq 1.4$$

where $\sigma_{t\ acs}$ = Anchor casing tensile strength [psi];
$\sigma_{c\ rcs}$ = Rising casing compressive strength [psi].

The axial loading of uncemented liners is caused by their weight because they are suspended in tension from a liner hanger or supported at the bottom of the well in compression.

The thermal or pressure-effect may produce a compressive load that transforms from helical buckling in an open hole. The helical buckling, $f_c$, is:

$$f_c = L_z \times W_P \times g \times [\frac{1}{A_p} + \frac{De}{2I_p}] \tag{10}$$

where $f_c$ = Total extreme fibre compressive stress due to axial and bending force [MPa];
$L_z$ = Total vertical length of liner or casing [m];
$W_P$ = Nominal unit weight of casing in air [kg/m];
$D$ = Casing outside diameter [mm];
$e$ = Eccentricity [mm];
$A_p$ = Cross-sectional area of casing wall [mm$^2$];
$I_p$ = Net moment of inertia of the pipe section [mm$^4$].

The design factor is:

$$\frac{\sigma_y \times Rj}{\sigma_c} \geq 1$$

where $\sigma_y$ = Minimum material yield stress [psi];
$R_j$ = Connection efficiency in compression (does exceed 1.0); and
$\sigma_c$ = Total compressive stress [psi].

### 3.2.3 Hoop and radial stress

The cementing of the well is done for sealing and support between the casing and the wall of the hole. Therefore, during cementing the well design shall ensure an adequate safety margin against yield arising from a high internal fluid pressure. The maximum differential internal pressure is:

$$\Delta P_{int} = \left[L_Z \rho_C - L_f \rho_f\right] \times g \times 10^{-3} \tag{11}$$

where $\Delta P_{int}$ = Differential pressure on casing during cementing [MPa];
$\rho_C$ = Cement slurry density [kg/l];
$L_f$ = Total vertical length of a fluid column in an annulus [m]; and
$\rho_f$ = Density of fluid, usually water, in the wellbore or annulus [kg/l].

The design factor is

$$\frac{P_y}{\Delta P_{int}} \geq 1.5$$

where $P_y$ = Internal yield pressure [MPa].

The $\rho_f$ is the density of water at temperature 50°C and it is equal 0.988.

The second maximum differential internal pressure appears at the surface and is the difference between the surface pressure and the wellhead pressure. It is evaluated after cementing has taken place by:

$$\frac{P_y \times Ri}{P_w} \geq 1.8$$

where $P_y$ = Internal yield pressure [MPa];
$Ri$ = Temperature reduction factor [ratio]; and
$P_w$ = Wellhead pressure [MPa].

The permanent wellhead is placed after cementing all the casings and then a biaxial stress condition exists that is the combined effects of the axial and circumferential tension. The wellhead is fixed at the 13-3/8" anchor casing. The following expression is used to calculate the combined effects of the axial and circumferential tension:

$$f_t = \frac{\sqrt{5}}{2} \times \frac{P_w d}{(D-d)} \tag{12}$$

where $f_t$ = Maximum tensile stress [MPa];
$D$ = Casing outside diameter [mm]);
$d$ = Casing inside diameter [mm].

The design factor is:

$$\frac{\sigma_{ys}}{f_t} \geq 1.5 \tag{13}$$

where $\sigma_{ys}$ = Steel yield strength [psi].

Collapse of the casing can be induced by external pressure from entrapped liquid expansion, or applied pressure of static pressure from a heavy liquid column such as cement slurry. During the later stage of the casing cementing operation, when the casing annulus is filled with dense cement slurry and the casing filled with water the maximum differential internal pressure is:

$$\Delta P_{ext} = [L_Z \rho_C - L_Z \rho_f] \times g \times 10^{-3} \tag{14}$$

where $\Delta P_{ext}$ = Differential external pressure [MPa].

The design factor is:

$$\frac{P_{pc}}{\Delta P_{ext}} \geq 1.2$$

where $P_{pc}$ = Pipe collapse pressure [MPa].

During production, the maximum external differential pressure occurs near the casing shoe when the annulus is at formation pressure ($P_Z$=$P_f$).

$$\frac{P_{pc}}{\Delta P_{ext}} \geq 1.2$$

## 4. WELLHEAD SELECTION

The permanent wellhead is the upper part of the well at the surface that is attached vertically to the top of the casing and is composed of the casing head flange, the master valve and the side valve (Figure 11). Its purpose is to control the fluid flow from the well. The two main designs of the wellhead are either that the casing head and master valve are attached directly to the production casing or an expansion spool, where the casing head is attached to the anchor casing and the wellhead built up from there (Thórhallsson, 2003).

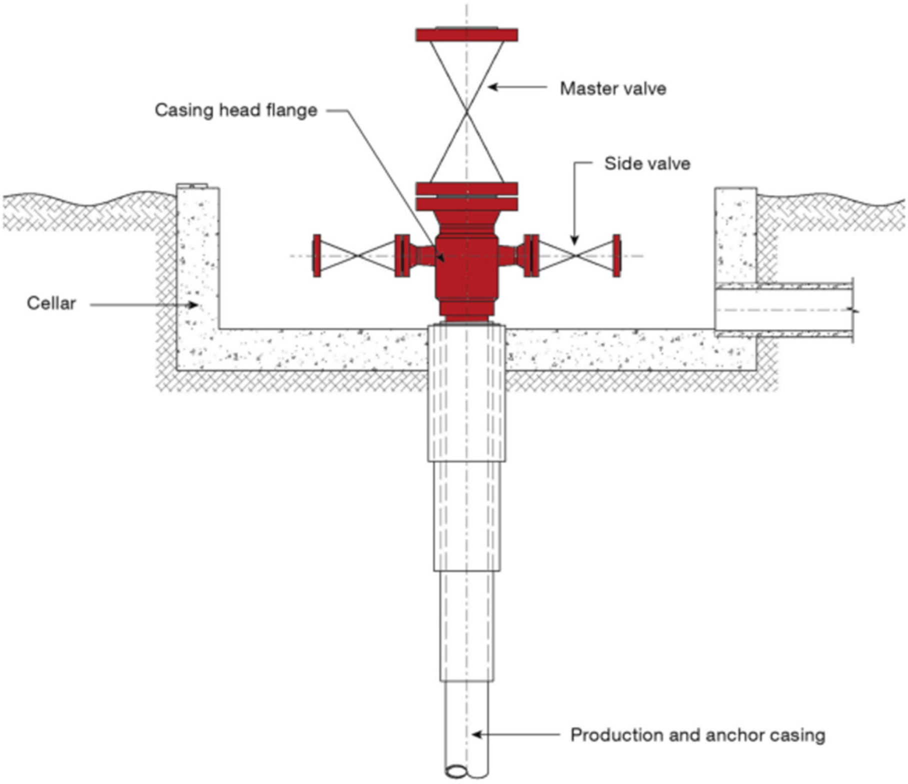


FIGURE 11: Typical permanent wellhead (African Union, 2016)

The wellhead of GLC-2 is designed to withstand the maximum design pressure for the corresponding hole section and temperature. The maximum pressure and temperature are 144 bar (14 MPa) and 336°C, respectively, and were used to select the wellhead pressure class ANSI 1500 (Figure 12). The temperature is the saturation temperature at 144 bar, taken from steam tables for pure water (Figure 9).

## 5. RESULTS

Table 2 shows the results of the axial loading analysis before and during cementing. During analysis it was assumed that casing is full of cement and the annulus full of water.

TABLE 2: The hookhand force of any casing section

| Casing diameter | Grade | Minimum tensile strength (kN) | F-hookhand (kN) | Calculated design factor | Minimum design factor |
|---|---|---|---|---|---|
| 9⅝” | K-55 | 3070 | 883.70 | 3.4 | 1.8 |
| 13⅜” | K-55 | 4760 | 919,82 | 5.2 | 1.8 |
| 20” | K-55 | 6590 | 985,48 | 6.7 | 1.8 |

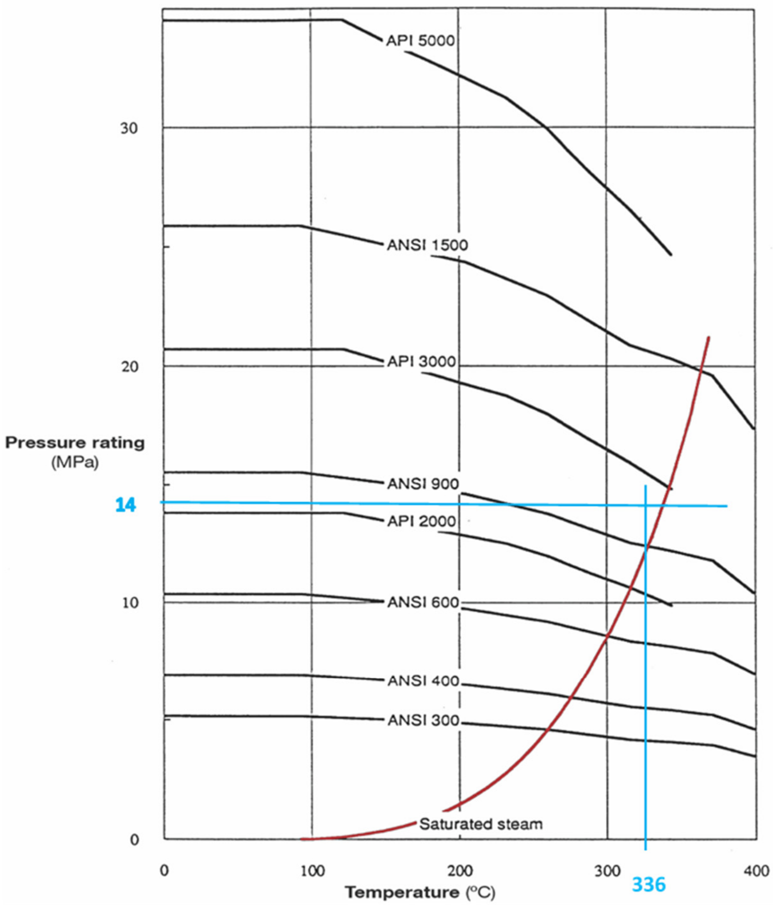


FIGURE 12: Wellhead working pressure de-rating for temperature (African Union, 2016) and maximum wellhead conditions (in blue)

The tension occurring at the top of the string that anchors the wellhead is computed as in Table 3.

TABLE 3: The fluid lifting force on the anchor casing

| Casing diameter | Maximum wellhead pressure, $P_w$ (MPa) | Net downward force on the wellhead, $F_m$ (kN) | Lifting force due to wellhead pressure, $F_w$ (kN) | Minimum tensile strength (kN) | Calculated design factor | Minimum design factor |
|---|---|---|---|---|---|---|
| 13⅜” | 14.4 | 22.36 | 1101.42 | 4760 | 4.3 | 1.8 |

The change in axial force due to temperature rise for different casings is computed in Table 4.

TABLE 4: The thermal load of all casing sections

| Casing diameter | $F_c$ (kN) | Rising casing compressive strength $F_r$ (kN) | Minimum tensile strength (kN) |
|---|---|---|---|
| 9⅝” | -0.0193 | 883.68 | 3070 |
| 13⅜” | -0.0294 | 919.79 | 4760 |
| 20” | -0.0475 | 985.43 | 6590 |

The compressive stress on uncemented liners due to self-weight and helical buckling is computed in Table 5.

TABLE 5: The helical buckling of the liner, compression

| Casing diameter | fc (MPa) | Rj | Minimum yield strength (MPa) | Calculated design factor | Minimum design factor |
|---|---|---|---|---|---|
| 7” | 146.27 | 1 | 379 | 2.59 | 1 |

The compressive stress on uncemented liners due to self-weight and helical buckling considering the temperature reduction factor is computed in Table 6.

TABLE 6: The helical buckling of the liner, compression with temperature de-rating.

| Casing diameter | fc (MPa) | Rj | Ri | Minimum yield strength (MPa) | Calculated design factor | Minimum design factor |
|---|---|---|---|---|---|---|
| 7” | 146.27 | 1 | 0.74 | 379 | 1.92 | 1 |

The maximum differential internal pressure of different casings is computed in Table 7.

TABLE 7: The internal pressure of all casing sections

| Casing diameter | Lz (m) | Differential internal pressure (MPa) | Internal yield pressure (MPa) | Calculated design factor | Minimum design factor |
|---|---|---|---|---|---|
| 9⅝” | 1110 | 6.85 | 42 | 6.13 | 1.5 |
| 13⅜” | 680 | 4.20 | 23.8 | 5.67 | 1.5 |
| 20” | 420 | 2.60 | 14.5 | 5.59 | 1.5 |

The maximum differential internal pressure occurring on the surface of the anchor casing is computed in Table 8. The temperature reduction factor is 0.74 and the wellhead pressure is 14.4 MPa.

TABLE 8: Internal differential pressure at the surface of the anchor casing

| Casing diameter | Temperature saturation (m) | Ri | Wellhead pressure (MPa) | Internal yield pressure (MPa) | Calculated design factor | Minimum design factor |
|---|---|---|---|---|---|---|
| 13⅜” | 366 | 0.74 | 14.4 | 39 | 2.06 | 1.8 |

The combined effects of the axial and circumferential tension is computed in Table 9.

TABLE 9: The wellhead internal pressure (wellhead is fixed)

| Casing diameter | Maximum tensile stress $f_t$ (MPa) | Wellhead pressure (MPa) | Steel yield strength (MPa) | Calculated design factor | Minimum design factor |
|---|---|---|---|---|---|
| 13⅜” | 202.26 | 14.4 | 621 | 3.07 | 1.5 |

The maximum differential external pressure will occur at the casing shoe when the casing annulus is filled with dense cement slurry. The external differential pressure for different casing strings is computed in Table 10.

TABLE 10: The external pressure collapse during cementing

| Casing diameter | Lz (m) | Differential external pressure (MPa) | Pipe collapse pressure (MPa) | Calculated design factor | Minimum design factor |
|---|---|---|---|---|---|
| 9⅝” | 1110 | 6.84 | 22.4 | 3.27 | 1.5 |
| 13⅜” | 680 | 4.19 | 13.4 | 3.19 | 1.5 |
| 20” | 420 | 2.59 | 3.6 | 1.38 | 1.5 |

During production, the maximum external differential pressure occurs near the casing shoe. The pressure is 14 MPa and the design factor is computed in Table 11.

TABLE 11: The external pressure collapse during production

| Casing diameter | Lz (m) | Differential external pressure (MPa) | Pipe collapse pressure (MPa) | Calculated design factor | Minimum design factor |
|---|---|---|---|---|---|
| 9⅝” | 1110 | 14 | 22.4 | 1.6 | 1.2 |

After the analysis of different casing loads the proposed casing grades, nominal weights and sizes are listed in Table 12.

TABLE 12: Proposed casing design of the well at the Asal geothermal field in Djibouti

| Casing | Nominal size (“) | Steel grade | Weight (lb/ft) | Depth (m) |
|---|---|---|---|---|
| Surface | 20 | K-55 | 94 | 420 |
| Anchor | 13⅜ | K-55 | 68 | 680 |
| Production | 9⅝ | K-55 | 43,5 | 1110 |
| Liner | 7 | K-55 | 26 | 890 |

## 6. DRILLING PROGRAMME

The results were obtained by using the African Union Code of Pratice for Geothermal Drilling (African Union, 2016) for the Asal geothermal field. For a future well, named GLC-2, close to Asal-3, which is planned to a depth of 2000 m, the production casing shoe would have been set to a depth of approx. 1110 m, the anchor casing shoe to 680 m and the surface casing shoe to 420 m. A proposed generic drilling programme based on Willis and Clarence (1981) that can be used as basis for a drilling programme for well GLC-2 is shown below.

*Phase I. Conductor hole or pre-drilling.*

1. Drill a 12 ¼" pilot hole with mud to 160 m. Start pilot hole by centre punching inside existing 30" casing with a 26" hole opener and 12 ¼" pilot bit;
2. Open 12 ¼” hole to 17 ½" down to 160 m;
3. Open 17 ½" hole to 26" down to 140 m;
4. Bail mud out of hole down to 140 m;
5. Cut off 30" pipe at cellar floor and remove it;
6. Run 20" casing and cement; and
7. Nipple up flow-line and air drill head to 22" casing.

*Phase II. Surface hole.*

1. Drill a 17 ½" hole with mud to a depth of 410 m;

2. Bail hole until clear water is obtained. Take three, one gallon samples;
3. Run wireline water probe to establish water level if water is present. Enter results in daily report;
4. Run wireline temperature survey from top of water to bottom of hole and enter results on daily drilling report;
5. Finish drilling 17 ½" "pilot hole" with mud to 13 3/8" casing depth to a depth of 410 m (make 10 feet extra hole);
6. An attempt to establish full circulation with mud will be made;
7. Condition hole for running casing;
8. Run 13 3/8" casing;
9. Cement 13 3/8" casing;
10. Cut off 20" casing at cellar floor;
11. Cut off 13 3/8" casing and nipple up. Test the weld on 13 3/8" casing before nippling up blowout preventer (B.O.P) stack complete with choke manifold and kill lines;
12. Pressure test casing, choke manifold valve and flanges with blinds closed – 900 ANSI for 50 minutes. All pressure tests to be witnessed by state; and
13. Drill out with 12 ¼ " bit and water. Pressure test casing (900 ANSI for 50 minutes) after drilling out each tool. After drilling out cement to 10 m above the shoe, pressure test entire 13 3/8" casing at 900 ANSI for 50 minutes.

*Phase III. Anchor hole or intermediate hole.*

1. Drill a 12 ¼ " hole with mud;
2. Condition mud and hole for logging;
3. Condition hole for running 9 5/8" casing;
4. Lay down drill collar;
5. Run 9 5/8" casing
6. Cement 9 5/8" casing to surface, wait on cement (WOC) to be determined by retardation of cement, or minimum of 24 hours;
7. Cut off 9 5/8" casing, install an expansion spool, and lay down a 5" drill pipe. Install expansion spool and nipple up. Change pipe ram to 4";
8. Pressure test casing, well head flange, and choke manifold with blind rams closed.
9. Pick up 8 ¾"bit, 6 ¾" drill collars and 4" drill pipe;
10. Pressure test pipe rams and hydril - 900 ANSI for 50 minutes; and
11. Drill out all cementing staging tools with water, float collar, and cement to within 3 m of casing shoe. Pressure test after drilling 3 m above the cement shoe, at 1000 PSIG for 50 minutes.

*Phase IV. Production hole.*

1. Drill out cement and casing shoe with 8 ¾" bit, rerun Mill tooth bit by passing all contaminated mud to reserve pit;
2. Drill 8 ¾" hole with TCI bits to total depth with mud;
3. Test after reaching a minimum temperature of 200°C, as indicated by drilling break or lost circulation;
4. Condition hole for logs; and
5. Run logs (confirmation reservoir) and assess if further hole drilling is required.

*Phase V. Production test.*

1. Displace mud in hole with water using 4" drill pipe (no collars) float bit sub and 8 ¾" bit bottom of 9 5/8" casing;
2. Using high-pressure air compressor, depress fluid in the hole to the bottom of the 9 5/8" casing. Shut in the well and let the fluid heat up to 100°C;
3. Flow test well after releasing the pressure out of the choke line and flow the well;
4. Kill/cool well with water;
5. Check depth and clean out to bottom with drill string;
6. Lay down drill pipe and tools; and
7. Close gate valve, remove B.O.P. stack and nipple up geothermal wellhead.

## 7. DISCUSSION

The chosen material grade of the surface casing, anchor casing, production casing and slotted liner, API K55, is recommended for geothermal conditions.

For assessing the axial loading before and during cementing, the calculated design factors for the tensile force of the 20" surface casing, 13⅜" anchor casing and 9⅝ production casing, were calculated as 6.68, 5.17 and 3.4, respectively. These design factors are all above the minimum design factor of 1.8.

The design factor considering the internal pressure during cementing of anchor and production casings that could burst the surface casing, was computed as 5.6 for the 20" surface casing, 5.7 for the 13⅜" anchor casing and 6.1 for the 9⅝ production casing. All the casings were adequate as the minimum design factor from the standard is 1.5.

The computed design factor for the production casing, considering the external differential pressure at the shoe, is 1.6 while the minimum design factor is 1.2, hence a 9⅝" 43.5 lb/ft K55 casing is adequate.

Scaling is expected due to the high salinity of the reservoir fluid. Preventive measures need to be defined and could be accomplished several ways. Inhibitor tests are aimed at preventing metal sulphide scaling by deactivating the metal ions and thus preventing the formation of sulphides as well as of chloride complexes thought to act as a catalyst to silica deposition at high temperature, and thus indirectly preventing silica scaling as well (Virkir-Orkint Consulting Group Ltd, 1990). Setting a high operation pressure of the wells could also reduce scaling within the well, depending on fluid chemistry.

## 8. CONCLUSIONS

The well design of the well that is planned to be drilled close to wells Asal-3 and Asal-6, that were drilled in 1989, was described. Production tests from these wells show a high flow, but very saline fluid of about 120 g/l. For the new planned GLC-2 well, the minimum casing depths were determined from the stratigraphy of the Asal 3 well and the BPD curve (12 wt% NaCl) with a great consideration to extend the casing lifetime.

After determination of the minimum casing depths, an evaluation of the casing stresses, i.e. axial stresses, radial stresses and hoop stresses, was carried out according to methods given in the African Union Code of Practice for Geothermal Drilling (African Union, 2016).

For the well design of the GLC-2 well, the result of each individual stress was based on the method specified in the African Union Code of Practice for Geothermal Drilling (African Union, 2016). The casings were chosen according to the criteria of design factors being higher than the specified minimum design factor for each load case of the casing. Minimizing scaling deposition inside the well has been outside of the scope of this report but scaling mitigation in the area calls for a special study.

## ACKNOWLEDGEMENTS

I would like to thank all the staff of the United Nations University, Geothermal Training Programme, Mr. Lúdvík S. Georgsson, Director of UNU-GTP, Ms. Málfrídur Ómarsdóttir. Mr. Ingimar G. Haraldsson, Mr. Markús A.G. Wilde, Mr. Ingimar G. Haraldsson and Ms. Þórhildur Ísberg for their guidance and support during my stay in Iceland.

I wish to express my gratitude to my supervisor, Mr. Gunnar Skúlason Kaldal. This report could not have been completed without his guidance and input. I would also like to thank all my teachers at UNU-GTP, as well as all the 2018 UNU Fellows for their friendship and fellow feeling, in particular Mr. Rufus Maina.

Finally, I would also like to thank my parents.

## REFERENCES

African Union, 2016: *Code of practice for geothermal drilling*. African Union, Regional Geothermal Coordination Unit, 150 pp.

Ali, B., 2015: Project evaluation of geothermal resources. *Proceedings of the World Geothermal Congress 2015, Melbourne, Australia*, 8 pp.

Aquater, 1987: *Well testing Asal 3 well.* Djibouti. Aquater, report, 26 pp.

Aquater, 1989: *Djibouti geothermal exploration project Republic of Djibouti, final report.* Aquater, report, 159 pp.

Árnason, K., Eysteinsson, H., and Vilhjalmsson, A.M., 2008: *The Asal geothermal field, Djibouti. Geophysical surface exploration 2007–2008. ÍSOR* – Íslenskar orkurannsóknir, report ÍSOR-2008/019, for Reykjavík Energy Invest, 74 pp..

Bosch, B., Deschamp, M., Leleu, M., Lopoukhine, A., Marce, C, and Vilbert., 1974: The Lake Asal geothermal area (T.F.A.I.): Field results and experimental geothermal studies. BRGM, Djibouti, section 4 (in French), 383 pp.

Demange, J., and Puvilland, P., 1993: *Geothermal field of Asal Djibouti, synthesis of data.* Compagnie Francaise pour le Developpement de la Geothermie Et Des Energies Nouvelles, Orleans, 75 pp.

Elmi, H.D., 2005: Analysis of geothermal well test data from the Asal rift area, Republic of Djibouti. Report 6 in: *Geothermal Training in Iceland 2005*. UNU-GTP, Iceland, 21 pp.

Geologica, 2016: *Asal-Fiale geothermal project, planning, drilling and testing electricity for Djibouti: Conceptual model of the geothermal system for well targeting.* Geologica, Djibouti, 48 pp.

Jalludin, M., 2013: State of knowledge of the geothermal provinces of the Republic of Djibouti. *Papers presented at "Short Course VIII on Exploration for Geothermal Resources" organized by UNU-GTP, GDC and KenGen at Lake Bogoria and Lake Naivasha, Kenya,* UNU-GTP SC-17, 17 pp.

Maurer Engineering INC., 1993: *Triaxial stress analysis model (TRIAX1).* Maurer Engineering Inc, Houston, TR93-3, 24 pp.

Reykjavik Energy Invest., 2008: *Geothermal exploration of Asal, Djibouti, drilling and testing.* Reykjavik Energy Invest, Djibouti, E2050, 59 pp.

Thórhallsson, S., 2003: Geothermal well operation and maintenance. *Lectures on sustainable use and operating policy for geothermal resources and papers presented at the International Geothermal Conference IGC2003 "Multiple integrated uses of geothermal resources" Reykjavik, 25th Anniversary Workshop of UNU-GTP, Iceland,* 23 pp.

Virkir-Orkint 1990: *Geothermal scaling and corrosion study, final report.* Virkir-Orkint Consulting Group Ltd, Djibouti, 273 pp.

Willis, R. and Clarence, J., 1981: *Geothermal drilling program.* Barnwell Geothermal Corporation, Water Resources International Inc., 69 pp.